Biological Cybernetics (2019) 113:257–271
https://doi.org/10.1007/s00422-019-00793-x

Biological Cybernetics

ORIGINAL ARTICLE

Extracellular GABA assisting in organizing dynamic cell assemblies to shorten reaction time to sensory stimulation

Ryuta Sakamoto[1] · Rikiya Kameno[2] · Taira Kobayashi[1] · Asahi Ishiyama[3] · Kazuo Watanabe[2] · Osamu Hoshino[1,2]

Received: 28 May 2018 / Accepted: 4 February 2019 / Published online: 12 February 2019

Abstract

Until recently, glia, which exceeds the number of neurons, was considered to only have supportive roles in the central nervous system, providing homeostatic controls and metabolic supports. However, recent studies suggest that glia interacts with neurons and plays active roles in information processing within neuronal circuits. To elucidate how glia contributes to neuronal information processing, we simulated a sensory neuron–glia (neuron–astrocyte) network model. It was investigated in association with ambient (extracellular) GABA level, because the astrocyte has a major role in removing extracellular GABA molecules. In the network model, transporters, embedded in plasma membranes of astrocytes, modulated local ambient GABA levels by actively removing extracellular GABA molecules which persistently acted on receptors in membranes outside synapses and provided pyramidal cells with inhibitory currents. Gap-junction coupling between astrocytes mediated a concordant decrease in local ambient GABA levels, which solicited a prompt population response of pyramidal cells (i.e., activation of an ensemble of pyramidal cells) to a sensory stimulus. As a consequence, the reaction time of a motor network, to which axons of pyramidal cells of the sensory network project, to the sensory stimulus was shortened. We suggest that the astrocytic gap-junction coupling may assist in organizing dynamic cell assemblies by coordinating a reduction in local ambient GABA levels, thereby shortening reaction time to sensory stimulation.

Keywords Astrocytic gap junction · GABA transport · Ambient GABA · Sensory information processing · Reaction time

1 Introduction

Traditionally, information processing in the brain has been viewed as a neuronal performance. Namely, dynamic signaling of neurons (mostly neuronal spiking activity) has long been considered to be responsible for transferring and dealing with information. The brain also possesses non-neuronal cells known as glial cells. Until recently, glia, which exceeds the number of neurons, was considered to only have supportive roles in the central nervous system, providing homeostatic controls and metabolic supports. However, recent studies suggest that glia interacts with neurons and plays active roles in information processing within neuronal circuits (Pannasch and Rouach 2013; Perea et al. 2014).

Among glia, astrocyte is known to regulate neuronal spiking activity (Wang et al. 2012). Stimulation of astrocytes activated other astrocytes and produced persistent depolarization in neighboring neurons known as UP state, which resulted in high-frequency firing in a population of neurons (Poskanzer and Yuste 2016). High-frequency firing, including gamma oscillations at 30–80 Hz, has been considered to have a close link with perceptual information processing (Ray and Maunsell 2015). Tallon-Baudry (2009) suggested that gamma oscillatory synchrony over the visual cortex could be induced when perceiving an object.

Neurons form circuits via synaptic connections and communicate with each other by rapid electrical impulses (neuronal spikes). In contrast, astrocytes do not generate electrical impulses; however, they can communicate with each other via gap junctions. Gap junctions are aggregates of intercel-

Communicated by Benjamin Lindner.

✉ Osamu Hoshino
osamu.hoshino.507@vc.ibaraki.ac.jp

[1] Department of Intelligent Systems Engineering, Ibaraki University, 4-12-1 Nakanarusawa, Hitachi, Ibaraki 316-8511, Japan

[2] Southern Tohoku Research Institute for Neuroscience, Southern Tohoku General Hospital, 7-115, Yatsuyamada, Koriyama, Fukushima 963-8563, Japan

[3] Production Engineering HQ, TDK Corporation, 151, Aza-Maeda, Hirasawa, Nikaho-shi, Akita 018-0402, Japan

lular channels, which permit the transfer of ions and small molecules between cells. Gap-junctional channels are composed of connexins, hexamers of medium-sized families of integral proteins. Connexins allow for direct electrical communication between cells, where different connexin subunits provide different unitary channel conductance of about 50 pS to 60 pS, leading to gap-junctional conductance of about tens of nanosiemens between astrocyte pairs (Dermietzel et al. 1991).

Giaume et al. (2010) suggested that astrocytic networks mediated by gap junctions might have a role in regulating neuronal network activity. Astrocytes respond to neighboring neuronal activity and increase cytoplasmic Ca^{2+} concentration. This intracellular signal triggers the release of chemical substances such as glutamate, ATP and D-serine, which is called gliotransmission and modulates neuronal activity. Accumulating evidence suggests that astrocyte can regulate ambient (extracellular) GABA levels, thereby modulating neuronal circuits in a tonic manner. Inhibition of neurons in a tonic manner means that extracellular GABA molecules persistently inhibit the neurons by acting on extrasynaptic $GABA_A$ receptors (Yoon and Lee 2014). Our previous study (Hoshino et al. 2018) demonstrated that astrocytic gap-junction coupling coordinated local ambient GABA levels, thereby synchronizing neuronal activity and enhancing spike-timing-dependent synaptic plasticity (STDP).

We speculated that the astrocytic gap-junction coupling might have a significant impact on neuronal information processing as well. The purpose of our study is to examine whether and how the astrocytic gap-junction coupling affects perceptual decision making in association with ambient GABA level, because the astrocyte has a major role in removing extracellular GABA molecules. In a sensory neuron–astrocyte network model, dynamic cell assemblies express information about sensory features. Each cell assembly, comprising pyramidal cells, small and large basket cells and astrocytes, responds to one particular feature stimulus. Transporters, embedded in plasma membranes of astrocytes, modulate ambient GABA levels. Ambient GABA molecules act on receptors in membranes outside synapses and provide pyramidal cells with inhibitory currents in a tonic manner.

Here we show that the gap-junction coupling between astrocytes mediates a concordant decrease in local ambient GABA levels, which solicits a prompt population response of pyramidal cells (i.e., activation of an ensemble of pyramidal cells) to a sensory stimulus. As a consequence, the reaction time of a motor network, to which axons of pyramidal cells of the sensory network project, is shortened. We conclude that the astrocytic gap-junction coupling assists in organizing dynamic cell assemblies by coordinating a reduction in local ambient GABA levels, thereby shortening reaction time to sensory stimulation.

2 Methods

2.1 Neuron-astrocyte network structure

Figure 1a shows our neural network model. The model consists of a sensory network (N_S) and a motor network (N_M).

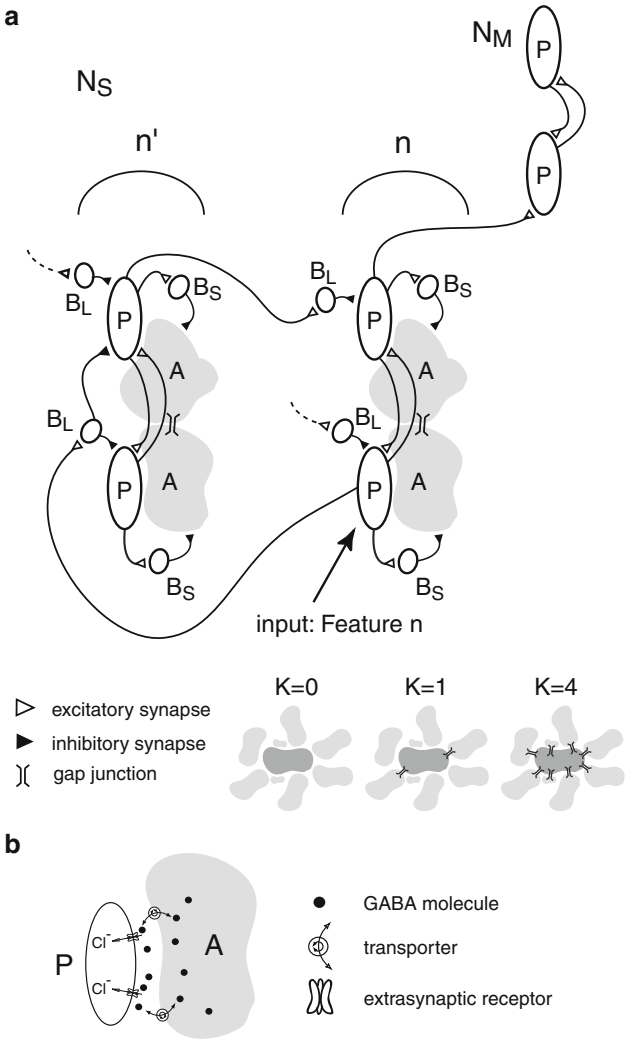

Fig. 1 Neuronal architecture. **a** The neural network model consisting of a sensory network (N_S) and a motor network (N_M). The N_S contains cell assemblies ($1 \leq n \leq 8$) with each comprising pyramidal cells (P), small and large basket cells (B_S, B_L), and astrocytes (A). The N_M contains a single-cell assembly (n) comprising P cells to which corresponding (n) N_S P cells project. Gap junctions connect neighboring A cells within cell assemblies. The open and filled triangles denote excitatory and inhibitory synapses, respectively. When the N_S is presented with a sensory stimulus (Feature n) as an input, a constant excitatory current is provided to corresponding (n) N_S P cells. Inset: Examples of astrocytic gap-junctional connectivity patterns: unconnected ($K = 0$), two connections ($K = 1$) and eight connections ($K = 4$). **b** A schematic illustration of GABA transport. Transporters on an A cell actively remove GABA molecules from the extracellular space when a B_S cell hyperpolarizes the A cell. Ambient (extracellular) GABA molecules are accepted by extrasynaptic $GABA_A$ receptors and tonically inhibit a P cell

The N_S contains cell assemblies with each comprising pyramidal cells (P), small and large basket cells (B_S, B_L) and astrocytes (A). Within the same cell assembly (n), each P cell receives excitatory and inhibitory inputs from P and B_L cells. Each B_S cell receives an excitatory input from its accompanying P cell, and each B_L cell receives excitatory inputs from P cells that belong to different cell assemblies ($n' \neq n$). Gap junctions connect neighboring A cells with each receiving an inhibitory input from a B_S cell. P cells belonging to cell assembly n receive an excitatory current as a sensory input when presented with a sensory stimulus: Feature n. The N_M detects the activation of N_S P cells that is induced by the sensory input and initiates a motor action, e.g., pressing a lever. N_M P cells are reciprocally connected with each other and receive input from corresponding (n) N_S P cells.

In a cortical three-dimensional space, astrocytes might connect with each other by gap junctions in a variety of connectivity patterns as is schematically illustrated in the inset of Fig. 1a. In each cell assembly, the ith A cell ($1 \leq i \leq 20$) was connected to no ($K = 0$), to two ($i-1, i+1$; $K = 1$) or to eight ($i-4, i-3, i-2, i-1, i+1, i+2, i+3, i+4$; $K = 4$) neighboring A cells. We employed a periodic boundary condition for astrocytic connections. Namely, the first ($i = 1$) A cell is adjacent to the last ($i = 20$) A cell. We will investigate in Sect. 3.1 how the gap-junctional connectivity pattern affects reaction time.

We employ here a gliotransmission mechanism (Hoshino 2009, 2012, 2014) in order to modulate local ambient GABA levels. Richerson and colleagues (Richerson and Wu 2003; Wu et al. 2003; Richerson 2004; Wu et al. 2007) indicated that the GABA transporter such as GAT-1 could operate in an ion-coupled manner. A thermodynamic reaction cycle involves coupled translocation of two Na^+ ions, one Cl^- ion and one uncharged GABA molecule under normal physiological conditions. The co-transported molecules ($2Na^+$, Cl^-, GABA) pass through the membrane together depending on the electrochemical potential that is the sum of the electropotential and the chemical potential. The electrochemical potential is 0 at an equilibrium point.

The reversal potential of the transporter is the equilibrium membrane voltage (electropotential) of the astrocyte (Wu et al. 2007). Forward transport (i.e., GABA import) occurs at astrocyte membrane potentials below the reversal potential, whereas reverse transport (i.e., GABA export) occurs above the reversal potential. To transport GABA molecules across the astrocytic membrane, we assume B_S-to-A synaptic signaling via $GABA_B$ receptors, because of predominant expression of $GABA_B$ receptor by astrocytes (Losi et al. 2014). Figure 1b schematically shows a transporter model, illustrating that GABA molecules are actively removed from the extracellular space by transporters when a B_S cell hyperpolarizes an A cell. Ambient GABA molecules act on extrasynaptic $GABA_A$ receptors and provide a P cell with tonic inhibitory current.

For the details of the model, especially for its biological justification, see our previous study (Hoshino et al. 2018). In numerical simulations, we used the Euler method to integrate model equations, which will be defined in the following sections, and used C language for programming. Time step size for numerical calculation was 10 microseconds.

2.2 Neuron model

Membrane potential of the ith N_S P cell that belongs to cell assembly n is defined by the following equations.

$$c_m^P \frac{d}{dt} v_{n,i}^P(t) = -g_m^P (v_{n,i}^P(t) - v_{rest}^P) + I_{n,i}^{PP}(t) + I_{n,i}^{PB_L}(t) + I_{n,i}^{ext}(t) + I_n^{\xi}(t), \quad (1)$$

$$I_{n,i}^{PP}(t) = -g_{AMPA}(v_{n,i}^P(t) - v_{AMPA}) \sum_{\substack{j=1 \\ j \neq i}}^{N} w_{n,ij}^{PP} r_{n,j}^P(t), \quad (2)$$

$$I_{n,i}^{PB_L}(t) = -g_{GABA_A}(v_{n,i}^P(t) - v_{GABA_A}) \sum_{j=1}^{N} w_{n,ij}^{PB_L} r_{n,j}^{B_L}(t), \quad (3)$$

$$I_{n,i}^{ext}(t) = -g_{GABA_A}(v_{n,i}^P(t) - v_{GABA_A}) \delta_P r_{n,i}^{ext}(t), \quad (4)$$

$$I_n^{\xi}(t) = I_{inp}, \quad (5)$$

where $I_{n,i}^{PP}(t)$ is an excitatory synaptic current from other P cells, $I_{n,i}^{PB_L}(t)$ an inhibitory synaptic current from B_L cells, $I_{n,i}^{ext}(t)$ an inhibitory nonsynaptic current mediated by ambient GABA via extrasynaptic receptors and $I_n^{\xi}(t)$ an excitatory input current. $w_{n,ij}^{PP}$ and $w_{n,ij}^{PB_L}$ are synaptic connection weights from the jth P and B_L cells to the ith P cell, respectively. $r_{n,j}^P(t)$ is the fraction of AMPA receptors in the open state triggered by presynaptic action potentials of the jth P cell. $r_{n,j}^{B_L}(t)$ is the fraction of intrasynaptic $GABA_A$ receptors in the open state triggered by presynaptic action potentials of the jth B_L cell. Ambient GABA molecules act on extrasynaptic $GABA_A$ receptors embedded in P cell membranes, thereby opening channels through which chloride ions flow into P cells. $r_{n,i}^{ext}(t)$ denotes the fraction of the channel opening, which ranges from 0 to 1 (normalized). δ_P denotes the amount of the embedded extrasynaptic $GABA_A$ receptors. c_m^P, g_m^P, g_{AMPA}, g_{GABA_A}, v_{rest}^P, v_{AMPA}, v_{GABA_A} and I_{inp} are constants defined in Table 1.

B_S and B_L cells are defined by

$$c_m^{\alpha} \frac{d}{dt} v_{n,i}^{\alpha}(t) = -g_m^{\alpha}(v_{n,i}^{\alpha}(t) - v_{rest}^{\alpha}) + I_{n,i}^{\alpha P}(t), \quad (\alpha = B_S, B_L) \quad (6)$$

$$I_{n,i}^{B_S P}(t) = -g_{AMPA}(v_{n,i}^{B_S}(t) - v_{AMPA}) w_{n,i}^{B_S P} r_{n,i}^P(t), \quad (7)$$

Table 1 List of parameters and their values

Symbol	Description	Value	Unit
c_{m}^{α}	Membrane capacitance for cell type α (α = P, B_S B_L, A, P_M)	$c_{\mathrm{m}}^{\mathrm{P}} = 500,\ c_{\mathrm{m}}^{\mathrm{B_S}} = 243,\ c_{\mathrm{m}}^{\mathrm{B_L}} = 115, c_{\mathrm{m}}^{\mathrm{A}} = 10, c_{\mathrm{m}}^{\mathrm{P_M}} = 500$	pF
g_{m}^{α}	Membrane conductance for cell type α (α = P, B_S B_L, A, P_M)	$g_{\mathrm{m}}^{\mathrm{P}} = 25,\ g_{\mathrm{m}}^{\mathrm{B_S}} = 9.7, g_{\mathrm{m}}^{\mathrm{B_L}} = 8.2, g_{\mathrm{m}}^{\mathrm{A}} = 20, g_{\mathrm{m}}^{\mathrm{P_M}} = 25$	nS
$v_{\mathrm{rest}}^{\alpha}$	Resting potential for cell type α (α = P, B_S B_L, A, P_M)	$v_{\mathrm{rest}}^{\mathrm{P}} = -65,\ v_{\mathrm{rest}}^{\mathrm{B_S}} = v_{\mathrm{rest}}^{\mathrm{B_L}} = v_{\mathrm{rest}}^{\mathrm{A}} = -70, v_{\mathrm{rest}}^{\mathrm{P_M}} = -65$	mV
g_{Z}	Maximal conductance for receptor type Z (Z = AMPA, $GABA_A$, $GABA_B$)	$g_{\mathrm{AMPA}} = 0.5, g_{\mathrm{GABA_A}} = 0.7, g_{\mathrm{GABA_B}} = 1$	nS
g_{GJ}	Maximal conductance for gap junction	20	nS
v_{Z}	Reversal potential for receptor type Z (Z = AMPA, $GABA_A$, $GABA_B$)	$v_{\mathrm{AMPA}} = 0, v_{\mathrm{GABA_A}} = -80, v_{\mathrm{GABA_B}} = -95$	mV
N	Number of cell units within cell assemblies	20	*
M	Number of cell assemblies	8	*
$w_{n,ij}^{\mathrm{PP}}$	Synaptic weight (strength) from j to i th P cell in cell assembly n	0.5	*
$w_{n,ij}^{\mathrm{PB_L}}$	Synaptic weight from j th B_L to i th P cell in cell assembly n	4	*
$w_{n,i}^{\mathrm{B_S P}}$	Synaptic weight from i th P to B_S cell in cell assembly n	40	*
$w_{nn',i}^{\mathrm{B_L P}}$	Synaptic weight from i th P to B_L cell between different ($n' \neq n$) cell assemblies	25	*
$w_{n,i}^{\mathrm{AB_S}}$	Synaptic weight from i th B_S to A cell in cell assembly n	25	*
$w_{n,ij}^{\mathrm{P_M P_M}}$	Synaptic weight from j to i th N_M P cell in cell assembly n	10	*
$w_{n,ij}^{\mathrm{P_M P}}$	Synaptic weight from j th N_S P cell to i th N_M P cell between corresponding cell assemblies: n	4.5	*
δ_{P}	Amount of extrasynaptic $GABA_A$ receptors on P cell	750	*
I_{inp}	Sensory input current	250	pA
α_{Z}	Channel opening rate for receptor type Z (Z = AMPA, $GABA_A$, $GABA_B$)	$\alpha_{\mathrm{AMPA}} = 1.1 \times 10^6,\ \alpha_{\mathrm{GABA_A}} = 5 \times 10^6,$ $\alpha_{\mathrm{GABA_B}} = 9 \times 10^4$	$\mathrm{M^{-1}s^{-1}}$
β_{Z}	Channel closing rate for receptor type Z (Z = AMPA, $GABA_A$, $GABA_B$)	$\beta_{\mathrm{AMPA}} = 190, \beta_{\mathrm{GABA_A}} = 180, \beta_{\mathrm{GABA_B}} = 1.2$	$\mathrm{s^{-1}}$
$\mathrm{Glu}_{\mathrm{syn}}^{\mathrm{P}}$	Intrasynaptic glutamate concentration for presynaptic P cell	1	mM
$\mathrm{GABA}_{\mathrm{syn}}^{\alpha}$	Intrasynaptic GABA concentration for presynaptic cell type α (α = B_S B_L)	$\mathrm{GABA}_{\mathrm{syn}}^{\mathrm{B_S}} = \mathrm{GABA}_{\mathrm{syn}}^{\mathrm{B_L}} = 1$	mM
l	The number of G-protein binding sites on K^+ channels	4	*
L_{ds}	Dissociation constant of G-protein binding	100	$\mu\mathrm{M}^4$
L_{ac}	G-protein activation rate	180	$\mathrm{s^{-1}}$
L_{da}	G-protein deactivation rate	34	$\mathrm{s^{-1}}$
η_{α}	Steepness of sigmoid function for cell type α (α = P, B_S B_L, P_M)	$\eta_{\mathrm{P}} = 260, \eta_{\mathrm{B_S}} = \eta_{\mathrm{B_L}} = 310, \eta_{\mathrm{P_M}} = 490$	$\mathrm{mV^{-1}}$
θ_{α}	Threshold of sigmoid function for cell type α (α = P, B_S B_L, P_M)	$\theta_{\mathrm{P}} = -40, \theta_{\mathrm{B_S}} = -37, \theta_{\mathrm{B_L}} = -34, \theta_{\mathrm{P_M}} = -34$	mV
K	Extent of astrocytic connectivity	1	*
γ_{trn}	Decay constant for ambient GABA concentration	3	$\mathrm{s^{-1}}$
$[\mathrm{GABA}]_0$	Basal ambient GABA concentration	1	μM
$\mathrm{GABA}_{\mathrm{max}}$	Maximal ambient GABA concentration	3.5	μM
$\mathrm{GABA}_{\mathrm{min}}$	Minimal ambient GABA concentration	0	μM
T_{G}	GABA transfer coefficient	2	$\mu\mathrm{M^{-1}mV^{-1}\,s^{-1}}$
$v_{\mathrm{rev}}^{\mathrm{A}}$	Reversal potential of astrocytic GABA transporter	-70	mV

*Unitless

$$I_{n,i}^{\mathrm{B_L P}}(t) = -g_{\mathrm{AMPA}}(v_{n,i}^{\mathrm{B_L}}(t) - v_{\mathrm{AMPA}}) \sum_{\substack{n'=1 \\ n' \neq n}}^{M} w_{nn',i}^{\mathrm{B_L P}} r_{n',i}^{\mathrm{P}}(t). \tag{8}$$

where $I_{n,i}^{\mathrm{B_S P}}(t)$ and $I_{n,i}^{\mathrm{B_L P}}(t)$ are excitatory synaptic currents from P cell(s). $w_{n,i}^{\mathrm{B_S P}}$ and $w_{nn',i}^{\mathrm{B_L P}}$ are P-to-B_S and P-to-B_L synaptic connection weights, respectively.

2.3 Receptor model and action potential generation

Receptor dynamics are defined by

$$\frac{\mathrm{d}}{\mathrm{d}t} r_{n,j}^{\mathrm{P}}(t) = \alpha_{\mathrm{AMPA}}[\mathrm{Glu}]_{n,j}(t)(1 - r_{n,j}^{\mathrm{P}}(t)) - \beta_{\mathrm{AMPA}} r_{n,j}^{\mathrm{P}}(t), \tag{9}$$

$$\frac{\mathrm{d}}{\mathrm{d}t} r_{n,j}^{\mathrm{B_S}}(t) = \alpha_{\mathrm{GABA_B}}[\mathrm{GABA}]_{n,j}^{\mathrm{B_S}}(t)(1 - r_{n,j}^{\mathrm{B_S}}(t)) - \beta_{\mathrm{GABA_B}} r_{n,j}^{\mathrm{B_S}}(t), \tag{10}$$

$$\frac{\mathrm{d}}{\mathrm{d}t} r_{n,j}^{\mathrm{B_L}}(t) = \alpha_{\mathrm{GABA_A}}[\mathrm{GABA}]_{n,j}^{\mathrm{B_L}}(t)(1 - r_{n,j}^{\mathrm{B_L}}(t)) - \beta_{\mathrm{GABA_A}} r_{n,j}^{\mathrm{B_L}}(t), \tag{11}$$

$$\frac{\mathrm{d}}{\mathrm{d}t} r_{n,j}^{\mathrm{ext}}(t) = \alpha_{\mathrm{GABA_A}}[\mathrm{GABA}]_{n,j}^{\mathrm{ext}}(t)(1 - r_{n,j}^{\mathrm{ext}}(t)) - \beta_{\mathrm{GABA_A}} r_{n,j}^{\mathrm{ext}}(t), \tag{12}$$

where $[\mathrm{Glu}]_{n,j}(t)$, $[\mathrm{GABA}]_{n,j}^{\mathrm{B_S}}(t)$ and $[\mathrm{GABA}]_{n,j}^{\mathrm{B_L}}(t)$ denote glutamate and GABA concentrations in synaptic clefts released from the jth P, B_S and B_L cells, respectively. $[\mathrm{GABA}]_{n,j}^{\mathrm{ext}}(t)$ denotes extracellular (ambient) GABA concentration around the jth P cell.

Probability of neuronal firing is defied by

$$PF_{n,j}^{\alpha} = \frac{1}{1 + \exp(-\eta_\alpha(v_{n,j}^{\alpha}(t) - \theta_\alpha))}. \qquad (\alpha = P, B_S, B_L) \tag{13}$$

$PF_{n,j}^{\alpha}$ denotes the probability of generating an action potential at time t. As will be shown in Sect. 3, in a raster plot, each line of bars is the activity of a single neuron with each bar indicating an action potential occurred at that time for the neuron.

A presynaptic neuron releases transmitter (glutamate or GABA) when an action potential arrives at the presynaptic terminal. The released transmitter then activates receptors on a postsynaptic neuron, by which ionic current flows into the postsynaptic neuron. Destexhe and colleagues (Destexhe et al. 1998) fitted the glutamate and GABA receptor models to postsynaptic currents obtained from whole-cell recordings, where they employed releases of 1 ms pulse of 1 mM glutamate and GABA into synaptic clefts. In our model, when firing, the membrane potential is depolarized to v_{act} (10 mV), kept for 1 ms, and then reset to the resting potential. This triggers a release of glutamate or GABA into the synaptic cleft, which is defined by

$$[\mathrm{Glu}]_{n,j}(t) = \mathrm{Glu}_{\mathrm{syn}}^{\mathrm{P}} H(v_{n,i}^{\mathrm{P}}(t) - v_{\mathrm{act}}), \tag{14}$$

$$[\mathrm{GABA}]_{n,j}^{\alpha}(t) = \mathrm{GABA}_{\mathrm{syn}}^{\alpha} H(v_{n,i}^{\alpha}(t) - v_{\mathrm{act}}). \qquad (\alpha = B_S, B_L) \tag{15}$$

In these equations, $\mathrm{Glu}_{\mathrm{syn}}^{\mathrm{P}}$ and $\mathrm{GABA}_{\mathrm{syn}}^{\alpha}$ are quantal discharges of glutamate and GABA molecules, respectively. H is a Heaviside function. The N_M P cell was similarly defined as the N_S P cell (not shown).

2.4 Astrocyte model

Dynamic evolution of membrane potential of the ith A cell that belongs to cell assembly n is defined by the following equations.

$$c_{\mathrm{m}}^{\mathrm{A}} \frac{\mathrm{d}}{\mathrm{d}t} v_{n,i}^{\mathrm{A}}(t) = -g_{\mathrm{m}}^{\mathrm{A}}(v_{n,i}^{\mathrm{A}}(t) - v_{\mathrm{rest}}^{\mathrm{A}}) + I_{n,i}^{\mathrm{AB_S}}(t) + I_{n,i}^{GJ}(t), \tag{16}$$

$$I_{n,i}^{\mathrm{AB_S}}(t) = -g_{\mathrm{GABA_B}}(v_{n,i}^{\mathrm{A}}(t) - v_{\mathrm{GABA_B}}) w_{n,i}^{\mathrm{AB_S}} \frac{([G]_{n,i})^l(t)}{([G]_{n,i})^l(t) + L_{\mathrm{ds}}}, \tag{17}$$

$$\frac{\mathrm{d}}{\mathrm{d}t}[G]_{n,i}(t) = L_{\mathrm{ac}} r_{n,i}^{\mathrm{B_S}}(t) - L_{\mathrm{da}}[G]_{n,i}(t), \tag{18}$$

$$I_{n,i}^{\mathrm{GJ}}(t) = \sum_{c=0}^{K} g_{\mathrm{GJ}}((v_{n,i-c}^{\mathrm{A}}(t) - v_{n,i}^{\mathrm{A}}(t)) + (v_{n,i+c}^{\mathrm{A}}(t) - v_{n,i}^{\mathrm{A}}(t))), \tag{19}$$

where $I_{n,i}^{\mathrm{AB_S}}(t)$ is an inhibitory synaptic current from a B_S cell, $I_{n,i}^{\mathrm{GJ}}(t)$ an electrical current from neighboring A cells and $w_{n,i}^{\mathrm{AB_S}}$ B_S-to-A synaptic connection weight. GABA activates $\mathrm{GABA_B}$ receptors indirectly. Namely, GABA binds to the receptor and activates it. The activated receptor catalyzes the activation of G-proteins. Finally, the activated G-proteins bind to the K^+ channel, leading to its opening (Destexhe et al. 1998). $[G]_{n,i}(t)$ is the concentration of activated G-proteins. In $([G]_{n,i})^l(t)$, l denotes the number of activated G-protein binding sites per channel; namely, the K^+ channel has l binding sites. L_{ds} denotes the dissociation constant of the binding of G-proteins on K^+ channels. L_{ac} and L_{da} denote the activation and deactivation rates of G-protein, respectively. K denotes the extent of connectivity across A cells and g_{GJ} the gap-junctional conductance.

2.5 GABA transporter model

The GABA transporter model controls local ambient GABA concentration, which is defined by

$$\frac{\mathrm{d}}{\mathrm{d}t}[\mathrm{GABA}]_{n,i}^{\mathrm{ext}}(t) = -\gamma_{trn}([\mathrm{GABA}]_{n,i}^{\mathrm{ext}}(t) - [\mathrm{GABA}]_0 + T_{\mathrm{G}}(\mathrm{GABA}_{\max} - [\mathrm{GABA}]_{n,i}^{\mathrm{ext}}(t))([\mathrm{GABA}]_{n,i}^{\mathrm{ext}}(t) - \mathrm{GABA}_{\min}) \times (v_{n,i}^{\mathrm{A}}(t) - v_{\mathrm{rev}}^{\mathrm{A}}). \tag{20}$$

In this equation, γ_{trn} is a decay constant, $[\text{GABA}]_0$ the basal ambient GABA concentration, T_{G} the modulation rate of ambient GABA concentration, GABA_{max} a maximum concentration, GABA_{min} a minimum concentration and $v^{\text{A}}_{\text{rev}}$ the reversal potential for GABA transport. All these parameter values are given in Table 1.

3 Results

3.1 Influence of astrocytic gap-junction coupling on perceptual information processing

To assess how astrocytic gap-junction coupling affects perceptual information processing, we ran two simulations in which adjacent astrocytes (A cells) were connected ($K = 1$) or not ($K = 0$). Figure 2a shows the reaction times (RTs) of the motor network (N_M) for $K = 0$ (top left) and for $K = 1$ (top right) when a sensory stimulus (Feature 4) was presented to the sensory network (N_S) (middle and bottom rows). RT measures a lapse of time between N_S stimulation and the beginning of N_M response. These results indicate that the gap junctions contribute to shortening the RT.

Figure 2b shows how A cells respond to the stimulus, indicating that the astrocytic gap-junction coupling hyperpolarizes a population of stimulus-sensitive ($n = 4$) A cells (bottom right), which is rapidly organized compared to that without coupling (bottom left). Note that the stimulus-sensitive ($n = 4$) cell assembly receives input current when presented with the sensory stimulus (Feature 4), whereas stimulus-insensitive ($n \neq 4$) cell assemblies do not. The stimulus-sensitive cell assembly was arbitrarily chosen. As shown in Fig. 2c (bottom right), the astrocytic gap-junction coupling promotes a prompt and concordant decrease in ambient GABA levels, thereby shortening the RT of N_M P cells (see the top-right panel of Fig. 2a). In contrast, without the coupling these A cell activities are desynchronized (see the bottom-left panel of Fig. 2b), and thereby, the hyperpolarization of some of the A cells happens to be delayed (e.g., see the arrow for $i = 17$; bottom left), which leads to a delay in removing GABA molecules around them (see the arrow for $i = 17$; bottom left in Fig. 2c), thereby prolonging the RT of N_M P cells (see the top-left panel of Fig. 2a).

To see how the astrocytic connectivity (K, Eq. (19)) affects the dynamic behavior of the network, we ran simulations in which different connectivity patterns were employed. As shown in Fig. 3a (left) where A cells were not connected ($K = 0$), adjacent A cells were connected ($K = 1$, triangles), six ($K = 3$, squares) or ten ($K = 5$, diamonds) nearest neighbors were connected, the gap-junction coupling shortens the RT, which is remarkable for weaker sensory stimuli ($<\sim$250 pA). The gain function of N_S P cells (i.e., input–output relationship), shown in Fig. 3a (right), indicates that the astrocytic gap-junction coupling does not affect the stimulus-evoked firing rate. This result implies that the shortening of RT does not arise from an increase in neuronal firing activity; i.e., the number of spikes evoked in N_S by the stimulus.

To elucidate how the gap-junction coupling leads to the shortening of RT, we recorded action potentials of N_S P cells. Figure 3b shows N_M (top) and N_S (middle) P cell responses (raster plots) where the gap-junction coupling did not exist (left) or existed (right). The bottom panels show averaged firing rates in a sliding window of 100 ms. It may be noted that the gap-junction coupling ($K = 5$) promotes N_S P cell firing at the stimulus onset (bottom right; see the dashed trace within the dashed circle), as compared to that without gap junctions ($K = 0$; see the solid trace within the dashed circle). These onset responses are transient, and shortly thereafter, they show almost identical stimulus-evoked firing activities (see the solid and dashed traces within the dashed rectangle). These results suggest that the shortening of RT of the N_M arises from a rapid organization of a stimulus-sensitive dynamic cell assembly through gap-junctional communication across astrocytes.

To understand how the prompt population response of N_S P cells (see the bottom-right panel of Fig. 2a) resulted in the shortening of the RT of N_M P cells (see the top-right panel of Fig. 2a), we recorded excitatory current flowing from N_S P cells into an N_M P cell. As shown in Fig. 4 (bottom), we found that the N_M P cell receives more excitatory current at the beginning of the persistent firings when the gap-junction coupling exists (dashed trace) than when it does not (solid trace). This result indicates that the prompt population response of N_S P cells quickly drives N_M P cells, thereby shortening their RT (see the top panel).

Then we asked whether partial input to the N_S could trigger a population neuronal response, which is evident in the primary visual cortex (Carrillo-Reid et al. 2016). To address this, we ran a simulation in which a portion (25 or 50 percent) of stimulus-sensitive P cells receives input current. As shown in Fig. 5a, b, the partial input can trigger a population neuronal response and the gap-junctional communication ($K = 5$) is essential for the shortening of RT. The relation between the RT and the fraction of stimulus-sensitive P cells receiving the input, shown in Fig. 5c, suggests that the astrocytic gap-junction coupling shortens the RT (circles) especially when the sensory input is sparse: less than 40%.

3.2 Minimization of negative consequences of sensory distraction on perceptual information processing by gap-junction coupling

To see how sensory distraction affects perceptual information processing, we ran a simulation in which the N_S was presented with a sensory stimulus (Feature 4) together

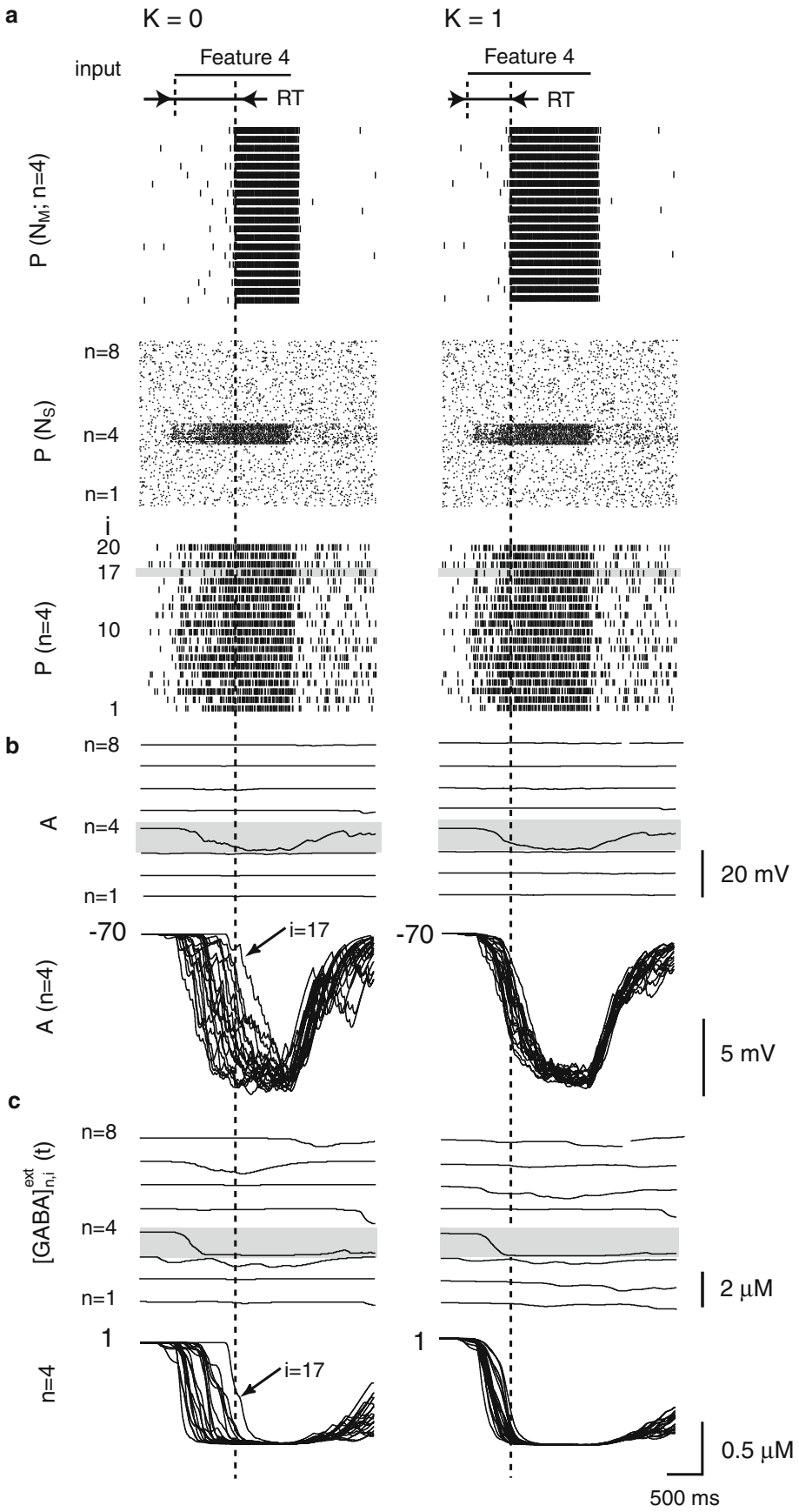

Fig. 2 Influence of astrocytic gap-junction coupling on perceptual decision making. **a** Top: Raster plots of stimulus-sensitive ($n = 4$) N_M P cells. Middle: Raster plots of N_S P cells belonging to different cell assemblies ($1 \leq n \leq 8$). Bottom: Raster plots of stimulus-sensitive ($n = 4$) N_S P cells. The gap-junction coupling did not exist ($K = 0$, left) or existed ($K = 1$, right). **b** A cell activity. Top: Membrane potentials of A cells belonging to different cell assemblies ($1 \leq n \leq 8$). Bottom: Overlaid representation of membrane potentials of 20 ($1 \leq i \leq 20$) stimulus-sensitive ($n = 4$) A cells. **c** Ambient GABA concentration. Top: Local ambient GABA concentrations around N_S P cells belonging to different cell assemblies ($1 \leq n \leq 8$). Bottom: Overlaid representation of local ambient GABA concentrations around 20 ($1 \leq i \leq 20$) stimulus-sensitive ($n = 4$) N_S P cells

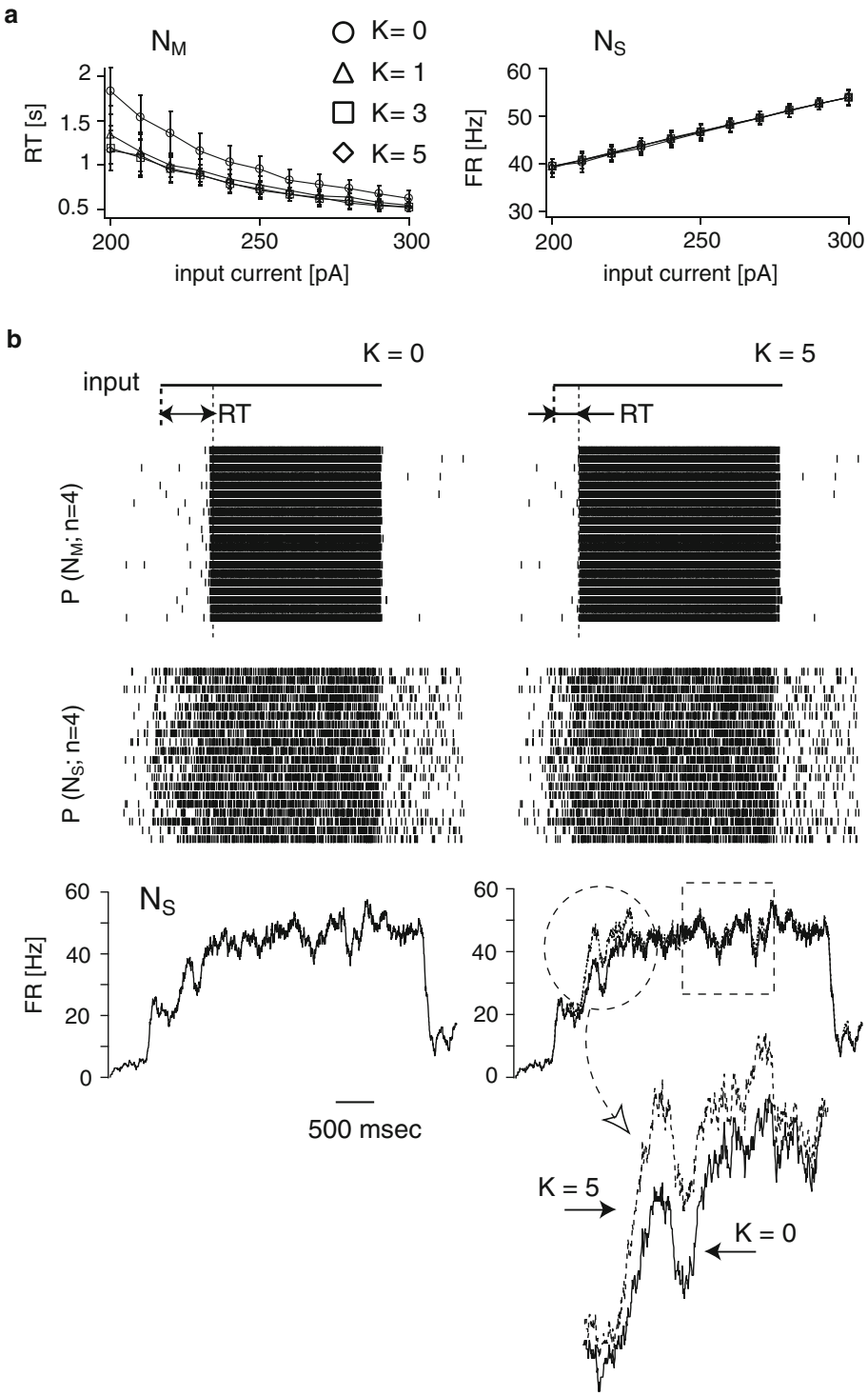

Fig. 3 Influence of astrocytic gap-junction coupling on reaction time. **a** Left: Relation between the RT of the N_M and sensory input current. The extent of astrocytic connectivity (K, Eq. (19)) was changed between 0 and 5. Right: The gain function (i.e., input–output relationship) of an N_S P cell. We implanted the same task repeatedly (20 trials) for each point. **b** N_M (top) and N_S (middle) P cell responses where the gap-junction coupling did not exist ($K = 0$, left) or existed ($K = 5$, right), and N_S P cell firing rates averaged in a sliding window of 100 ms (bottom)

with sensory distractors. These sensory distractors provide stimulus-insensitive pyramidal cells with small but significant currents, which we call distractor-induced noise current. We investigated how these distractors affect RT. As shown in Fig. 6 (left), the noise application prolongs the RT of N_M, as compared to that without noise (see the top-left panel of Fig. 2a). The deterioration of perceptual performance can be minimized if the gap-junction coupling is considered (top right). It may be noted that its RT is almost comparable to that without noise (see the top-left panel of Fig. 2a). These results suggest that the gap-junction coupling might be beneficial for promptly organizing the stimulus-sensitive dynamic cell assembly in the sensory cortex and thus for the shortening

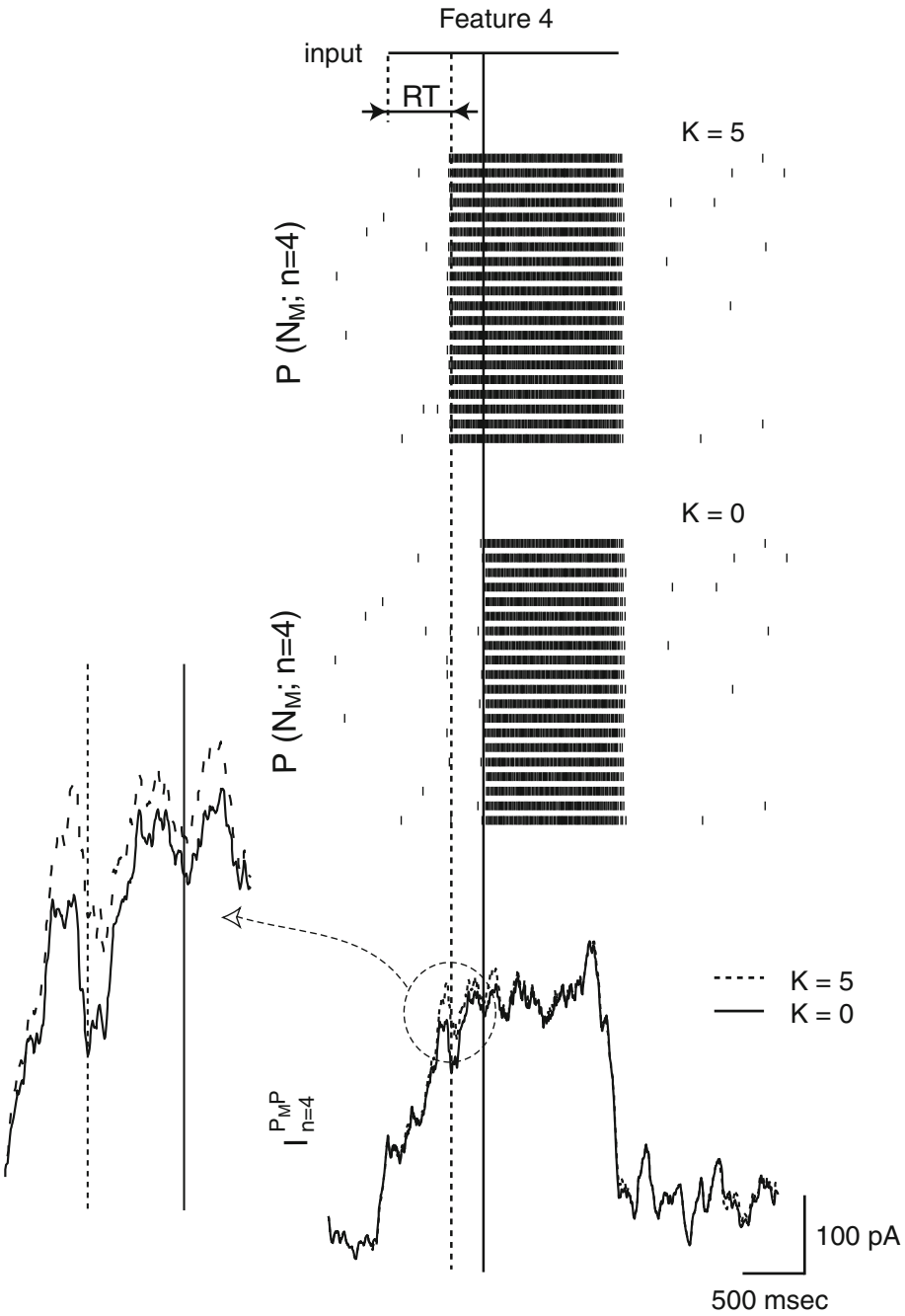

Fig. 4 Influence of astrocytic gap-junction coupling on motor cortex activity. Raster plots of stimulus-sensitive ($n = 4$) N_M P cells where the gap-junction coupling existed ($K = 5$, top) or not ($K = 0$, middle), and excitatory currents flowing from N_S P cells into an N_M P cell (bottom) where the gap-junction coupling existed (dashed trace) or not (solid trace)

of the RT of the motor cortex under the distractor-induced noisy environmental condition.

Then, we implemented a systematic analysis to elucidate how the gap-junction coupling shortens the RT under the distractor-induced noisy environmental condition. As shown in Fig. 7a (left), an increase in noise intensity delays the RT (squares) and an increase in the number of astrocytic gap-junction connection sites (K) shortens the RT. The shortening of RT by gap-junction coupling (right) is remarkable when the noise intensity is strong (squares). These results suggest that the astrocytic gap-junction coupling works to reduce the negative consequence of distractors in perceptual decision making, i.e., a delay in RT to sensory stimulation.

As shown in Fig. 6 (fourth), the prolonged RT might arise from an inharmonious hyperpolarization of A cells within the same cell assembly due to the lack of gap-junction coupling ($K = 0$, left). To elucidate how it leads to shortening the RT, we measured the times that were required to hyperpolarize A cells from -70 mV (resting potential) to -75 mV, which we termed hyperpolarization time (HT) and are shown in Fig. 7b (mean±SD, top left) as a function of (distractor-induced) noise current. This result indicates that the lack

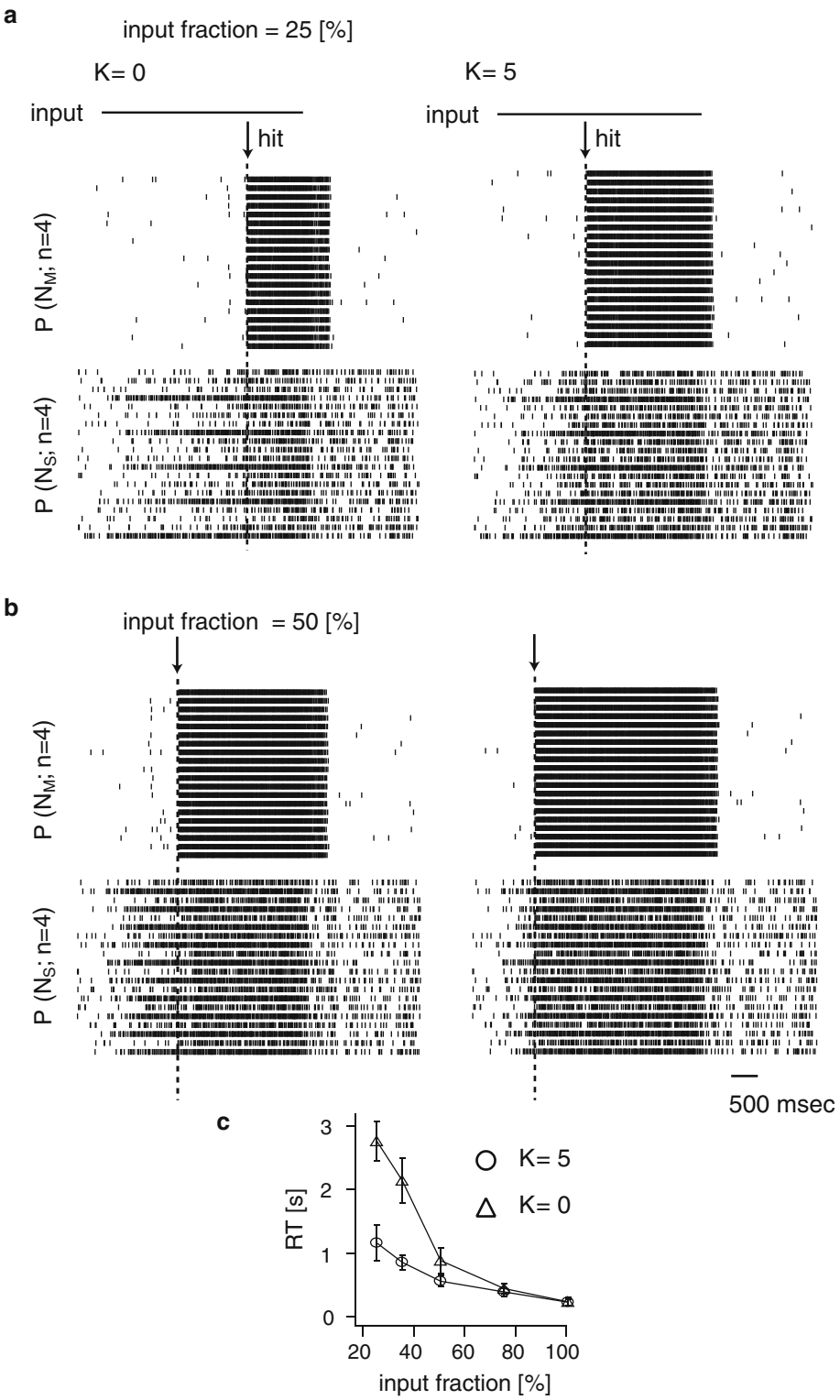

Fig. 5 Neuronal responsiveness to partial sensory input. **a** Raster plots of stimulus-sensitive ($n = 4$) N_M (top) and N_S (bottom) P cells. A portion (25 percent) of stimulus-sensitive P cells receives input current. We provided the same input without (left) or with (right) gap-junction coupling. **b** Those obtained under a condition in which the fraction of stimulus-sensitive P cells receiving the input current was 50 percent. **c** Relation between RT and input fraction. The gap-junction coupling existed (circles) or not (triangles)

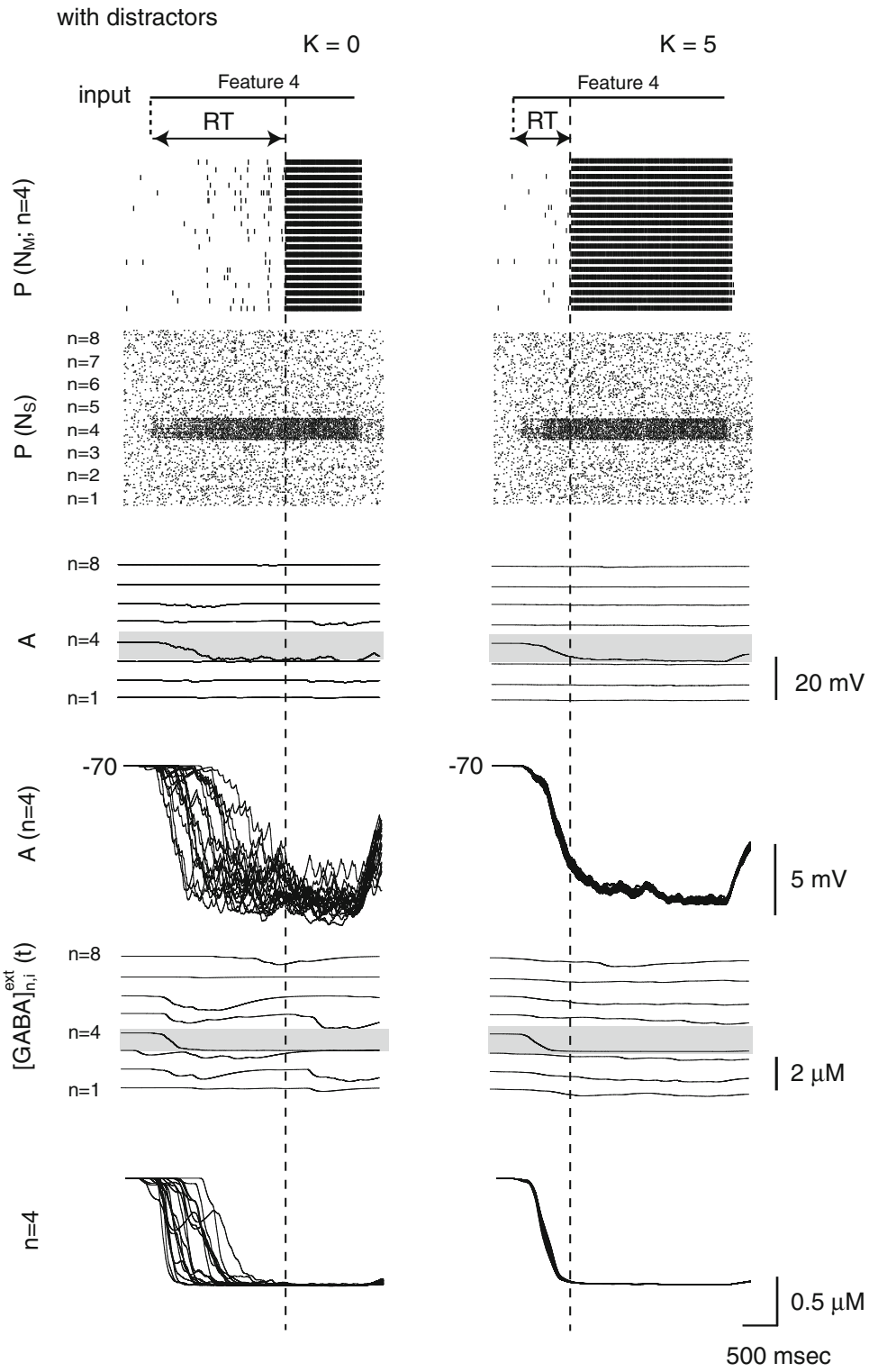

Fig. 6 Influence of sensory distraction on reaction time. Left: Raster plots of stimulus-sensitive ($n = 4$) N_M P cells (top), N_S P cells (second), membrane potentials of A cells (third) belonging to different cell assemblies ($1 \leq n \leq 8$), overlaid representation of membrane potentials of 20 ($1 \leq i \leq 20$) stimulus-sensitive ($n = 4$) A cells (fourth), ambient GABA concentrations around different ($1 \leq n \leq 8$) N_S P cells (fifth), and overlaid representation of ambient GABA concentrations around 20 ($1 \leq i \leq 20$) stimulus-sensitive ($n = 4$) N_S P cells (bottom). The gap-junction coupling did not exist ($K = 0$). Right: Those obtained under a condition in which the gap-junctional coupling existed ($K = 5$)

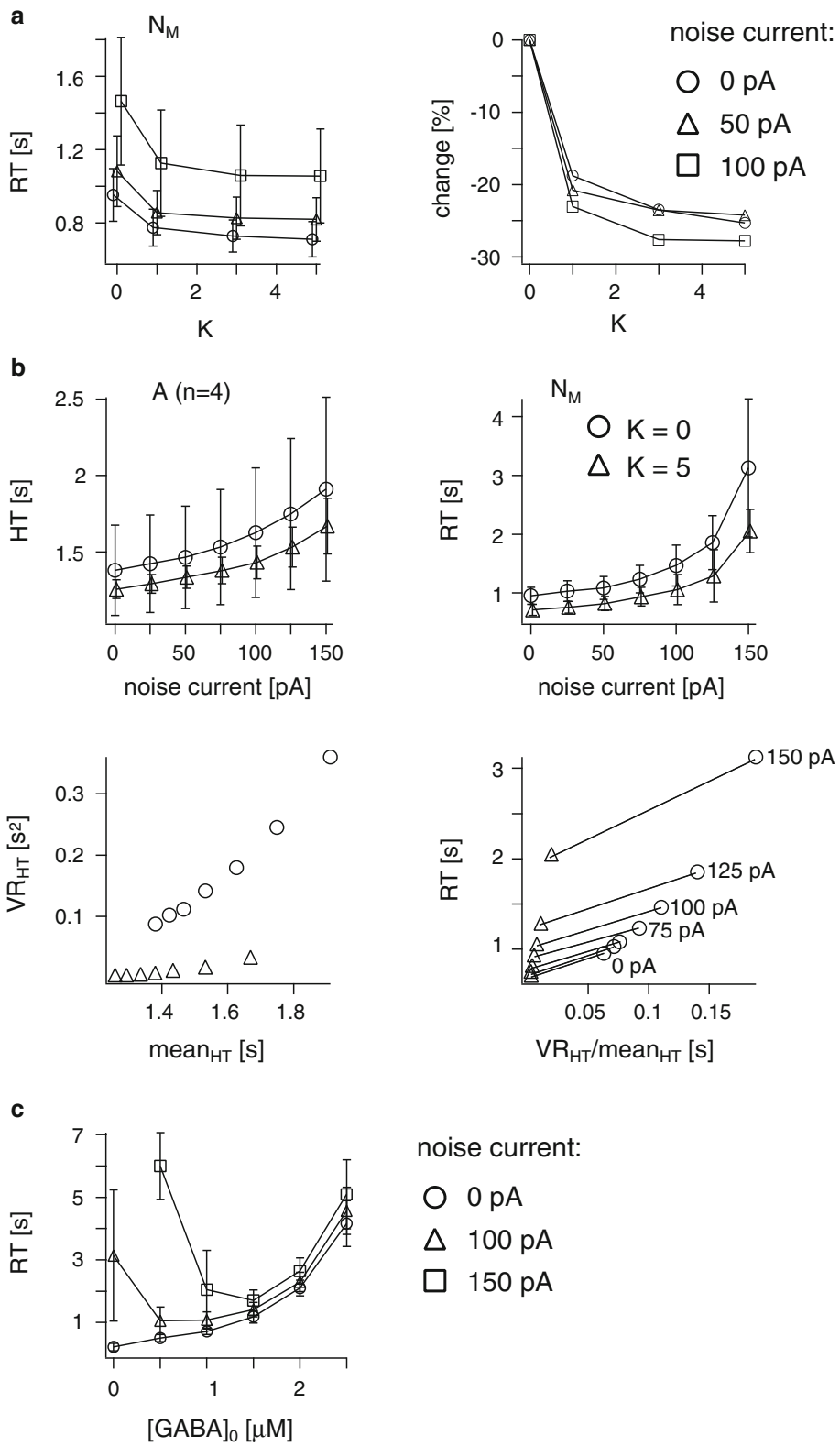

Fig. 7 Influence of astrocytic gap-junction coupling on reaction time under a distractor-induced noisy environmental condition. **a** Left: Dependence of RT of the N_M on astrocytic gap-junction connectivity (K). The intensity of noise was varied: 0 pA (circles), 50 pA (triangles), 100 pA (squares). Right: Shortening of RT by astrocytic gap-junction coupling. **b** Influence of variability in astrocyte membrane potential on RT. Top: Dependence of the time that is required to hyperpolarize A cells from the resting (-70 mV) to -75 mV (HT, left) and the RT (right) on noise intensity. Bottom: Relations between variance (VR_{HT}) and mean ($mean_{HT}$) (left) and between RT and $VR_{HT}/mean_{HT}$ (right). **c** Dependence of RT on basal ambient GABA level ($[GABA]_0$)

of gap-junction coupling ($K = 0$) is responsible for the delayed population (hyperpolarizing) response of A cells (circles). The bottom-left and top-right panels of Fig. 7b show the relations between its variance (VR_{HT}) and mean ($mean_{HT}$) and between RT and noise current, respectively. As shown in the bottom-right panel of Fig. 7b, we derived the relation between RT and $VR_{HT}/mean_{HT}$. This suggests that reducing the variability of astrocyte membrane potentials by gap-junction communication can shorten the RT.

We assumed the basal ambient GABA concentration ($[GABA]_0 = 1\mu M$ in Eq. (20)), which provided N_S P cells with persistent, tonic inhibitory current. As shown in Fig. 7c, such persistent tonic inhibition is unnecessary if the noise is not present (circles); rather, it prolongs the RT. However, it is vital when the sensory stimulus is present together with distractors (triangles, squares). We found an optimal ambient GABA level for each noise current: 0 pA at 0 μM, 100 pA at 0.5 μM and 150 pA at 1.5 μM where the RT could be maximally shortened. All these results indicate that the basal level of GABA in extracellular space is an important factor for perceptual decision making operated under the distractor-induced noisy environmental condition.

3.3 Robustness evaluation

To evaluate of the robustness of the network model, we changed the values of synaptic connection weight between P cells ($w^{PP}_{n,ij}$), gap-junctional conductance (g_{GJ}) and GABA transfer coefficient (T_G), and measured RT in association with the extent of astrocytic gap junctions (K). The relation between RT and $w^{PP}_{n,ij}$ is shown in Fig. 8a, where the extent of astrocytic connectivity was varied: $K = 0, 1, 3, 5$. This result indicates that the recurrent connections between pyramidal cells contribute to shortening the RT, and the extension of astrocytic gap-junction connectivity further shortens the RT. The relation between RT and g_{GJ} shown in Fig. 8b indicates that the gap-junctional conductance contributes to shortening the RT and that the extension of astrocytic gap-junction connectivity further shortens the RT. The relation between RT and T_G shown in Fig. 8c indicates that the active removal of GABA molecules from the local extracellular space contributes to shortening the RT and that the extension of astrocytic gap-junction connectivity further shortens the RT. Notably, we reached the same conclusion: astrocytic gap-junction connectivity contributes to shortening the RT.

4 Discussion

To investigate how gap-junction coupling between astrocytes affects perceptual information processing, we simulated a sensory neuron-astrocyte network model. It was investigated in association with ambient (extracellular) GABA level, because the astrocyte has a major role in removing GABA molecules from extracellular space. In the network model, transporters, embedded in plasma membranes of astrocytes, modulated local ambient GABA levels by actively removing extracellular GABA molecules which persistently acted on receptors in membranes outside synapses and provided pyramidal cells with inhibitory currents in a tonic manner. Gap-junction coupling between astrocytes mediated a concordant decrease in local ambient GABA levels, which solicited a prompt population response of pyramidal cells (i.e., activation of an ensemble of pyramidal cells) to a sensory stimulus. As a consequence, the reaction time of a motor network, to which axons of pyramidal cells of the sensory network project, was shortened. We suggest that the astrocytic gap-junction coupling may assist in organizing dynamic cell assemblies by coordinating a reduction in local ambient GABA levels, thereby shortening reaction time to sensory stimulation.

A study (Karnani et al. 2014) discussed overlapping inhibition by interneurons, called blanket inhibition. In general, GABAergic interneurons innervate nearby pyramidal cells without any apparent specificity as if they were extending a blanket of inhibition. It is well known that gap junctions often link inhibitory neurons to each other, and thereby, they can work as a unit (Yuste 2015). Thus, an interneuron network extends the blanket of inhibition onto excitatory pyramidal cells. It was suggested that as a result of blanket inhibition pyramidal cells could synchronize their spiking. Our study highlights that extracellular GABA can form a blanket of inhibition in a tonic manner and that the astrocytic gap-junction coupling contributes to making a hole in the tonic blanket inhibition by coordinating a reduction in local levels of GABA in extracellular space, which leads to a prompt population neuronal response to sensory stimulation.

Concerning a population response of pyramidal cells induced by partial input to the sensory network (see N_S in Fig. 5), a recent experiment (Carrillo-Reid et al. 2016) implemented repetitive, simultaneous activation of a population of pyramidal cells in the visual cortex. This treatment built neuronal ensembles, which could be recalled or induced by partial sensory stimulation, e.g., by single-cell stimulation. For the formation of cell assemblies, Hebbian plasticity works to strengthen synapses between pyramidal cells. Our study highlights that a transient reduction in local ambient GABA levels by transporters can assist in recalling dynamic cell assemblies embedded in network dynamics (i.e., for a dynamic cell assembly that is relevant to a sensory input to emerge), for which concordant hyperpolarization of astrocytes mediated by gap-junction coupling is essential.

It is well known that gap-junction coupled neurons contribute to synchronizing spiking activity, leading to generating the so-called gamma-band oscillation (Buzsaki and Wang 2012). We showed here that gap-junction coupled astrocytes

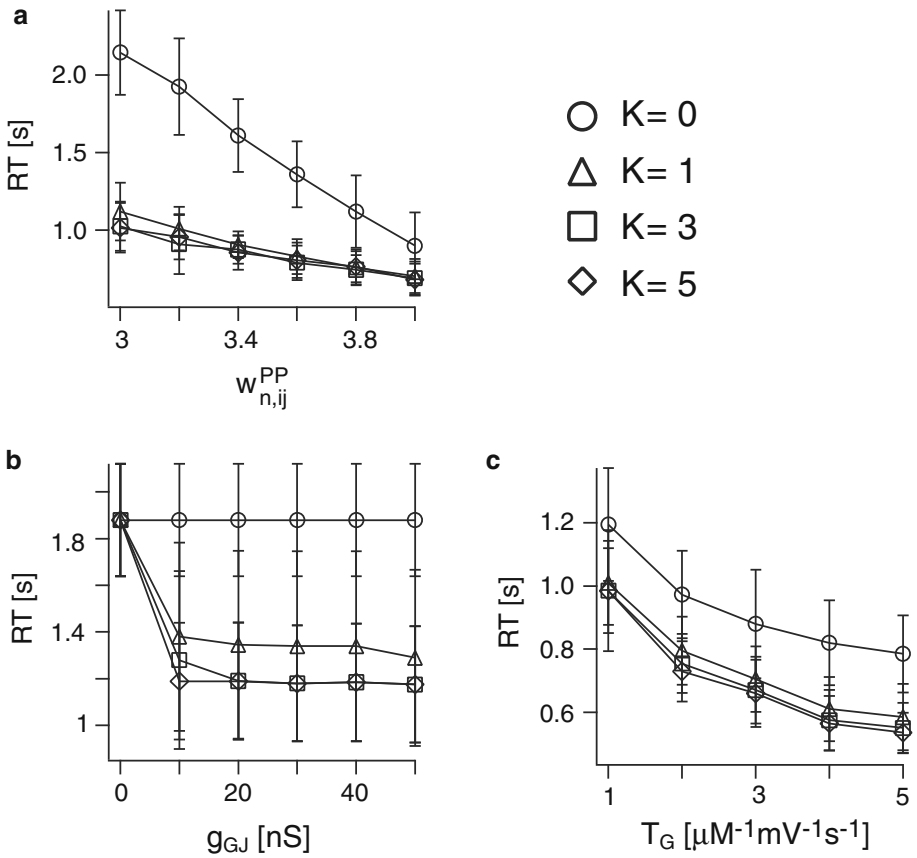

Fig. 8 Robustness evaluation. **a** Dependence of reaction time on synaptic connection weight between N_S P cells ($w^{PP}_{n,ij}$). The extent of astrocytic connectivity (K) was changed between 0 and 5. **b** Dependence of RT on gap-junctional conductance (g_{GJ}). **c** Dependence of RT on GABA transfer coefficient (T_G)

assisted in recalling a stimulus-sensitive dynamic cell assembly, thereby reducing the negative consequence of sensory distractors in perceptual decision making, i.e., a delay in reaction time to sensory stimulation. To the best of our knowledge, this is a novel finding.

References

Buzsaki G, Wang XJ (2012) Mechanisms of gamma oscillations. Annu Rev Neurosci 35:203–225

Carrillo-Reid L, Yang W, Bando Y, Peterka DS, Yuste R (2016) Imprinting and recalling cortical ensembles. Science 353:691–694

Dermietzel R, Hertberg EL, Kessler JA, Spray DC (1991) Gap junctions between cultured astrocytes: immunocytochemical, molecular, and electrophysiological analysis. J Neurosci 11:1421–1432

Destexhe A, Mainen ZF, Sejnowski TJ (1998) Kinetic models of synaptic transmission. In: Koch C, Segev I (eds) Methods in neuronal modeling. The MIT Press, Cambridge, pp 1–25

Giaume C, Koulakoff A, Roux L, Holcman D, Rouach N (2010) Astroglial networks: a step further in neuroglial and gliovascular interactions. Nat Rev Neurosci 11:87–99

Hoshino O (2009) GABA-transporter preserving ongoing-spontaneous neuronal activity at firing-subthreshold. Neural Comput 21:1683–1713

Hoshino O (2012) Regulation of ambient GABA levels by neuron-glia signaling for reliable perception of multisensory events. Neural Comput 24:2964–2993

Hoshino O (2014) Balanced crossmodal excitation and inhibition essential for maximizing multisensory gain. Neural Comput 26:1362–1385

Hoshino O, Zheng M, Watanabe K (2018) Improved perceptual learning by control of extracellular GABA concentration by astrocytic gap junctions. Neural Comput 30:184–215

Karnani MM, Agetsuma M, Yuste R (2014) A blanket of inhibition: functional inferences from dense inhibitory connectivity. Curr Opin Neurobiol 26:96–102

Losi G, Mariotti L, Carmignoto G (2014) GABAergic interneuron to astrocyte signalling: a neglected form of cell communication in the brain. Philos Trans R Soc Lond B 369:20130609

Pannasch U, Rouach N (2013) Emerging role for astroglial networks in information processing: from synapse to behavior. Trends Neurosci 36:405–417

Perea G, Sur M, Araque A (2014) Neuron-glia networks: integral gear of brain function. Front Cell Neurosci 8:378

Poskanzer KE, Yuste R (2016) Astrocytes regulate cortical state switching in vivo. Proc Natl Acad Sci USA 113:E2675–E2684

Ray S, Maunsell JH (2015) Do gamma oscillations play a role in cerebral cortex? Trends Cogn Sci 19:78–85

Richerson GB (2004) Looking for GABA in all the wrong places: the relevance of extrasynaptic GABA(A) receptors to epilepsy. Epilepsy Curr 4:239–242

Richerson GB, Wu Y (2003) Dynamic equilibrium of neurotransmitter transporters: not just for reuptake anymore. J Neurophysiol 90:1363–1374

Tallon-Baudry C (2009) The roles of gamma-band oscillatory synchrony in human visual cognition. Front Biosci 14:321–332

Wang F, Smith NA, Xu Q, Fujita T, Baba A, Matsuda T, Takano T, Bekar L, Nedergaard M (2012) Astrocytes modulate neural net-

work activity by Ca^{2+}-dependent uptake of extracellular K^{+}. Sci Signal 5:ra26

Wu Y, Wang W, Richerson GB (2003) Vigabatrin induces tonic inhibition via GABA transporter reversal without increasing vesicular GABA release. J Neurophysiol 89:2021–2034

Wu Y, Wang W, Diez-Sampedro A, Richerson GB (2007) Nonvesicular inhibitory neurotransmission via reversal of the GABA transporter GAT-1. Neuron 56:851–865

Yoon BE, Lee CJ (2014) GABA as a rising gliotransmitter. Front Neural Circuits 8:141

Yuste R (2015) From the neuron doctrine to neural networks. Nat Rev Neurosci 16:487–497